Mechanical and Swelling Behaviors of Rubber: A Comparison of Some Molecular Models with Experiment

WON HEE HAN
FERENC HORKAY
GREGORY B. MCKENNA
Polymers Division, National Institute of Standards and Technology, Gaithersburg, MD 20899, USA; gmckenna@nist.gov

(Received 1 June 1996; Final version 30 July 1998)

Abstract: A review is given of several current network models (constrained chain model, localization model, liquidlike model, and eight-chain model) that have been developed to explain nonideal rubbery behavior. The stress-strain relationships for both dry and swollen networks are discussed. It is shown that the constrained chain model of Flory, Erman, and Monnerie provides the best description of the considered models for the stress-strain response of both the dry state and swollen state properties of cross-linked rubber networks. The localization model of Gaylord and Douglas fits the dry-state stress-strain data very well, but the predictions of the mechanical response in the swollen state are not as good as those obtained with the constrained chain model. The liquidlike model of DiMarzio yields reasonable description of extension behavior, but it does not explain the observed modest decrease of the elastic modulus (reduced stress) with increasing compression; nor does the liquidlike model predict the decreasing modulus with increasing swelling correctly. The eight-chain model of Arruda and Boyce puts forward a stress-strain relation that includes the finite extensibility of the network chains. It is shown that at moderate deformation ratios, the eight-chain model does not provide even qualitative agreement with the experimental stress-strain data for both the dry and swollen states.

1. INTRODUCTION

Mechanical behavior of polymeric materials is a subject that is becoming increasingly important in the solid mechanics community with the result that, like mechanical metallurgy a half-century ago, there is an increasing attempt to extend concepts from condensed matter physics to the modeling of the stress-strain behavior of polymers [2, 4, 28, 42, 43, 49]. In doing so, it is important that the models so applied be evaluated not only for their description of the phenomenology at hand but for their ability to describe the original physical phenomena for which they were developed.

The current manuscript is motivated by the observation that, in recent years, there has been considerable interest in using rubber elasticity concepts to explain the large deformation response of glassy polymers in the postyield region [2, 28, 42, 49]. The argument that rubber elastic forces are significant contributors to the elastic back stress after yield is essentially as follows. Subsequent to yielding, the polymer undergoes large deformations. These deformations lead to alignment of the macromolecular network built of the entangled,

Mathematics and Mechanics of Solids, 4: 139-167, 1999

chainlike polymer molecules. The alignment of the network chains leads to entropic (rubbery) restorative forces that give rise to an elastic back stress. Sometimes strain hardening is observed, and this is often attributed to limited extensibility of the polymer chains in the network. Importantly, it has been assumed that the restorative forces (elastic back stress) can be modeled using rubber elasticity models.

The purpose of this paper, rather than to assess the plasticity models themselves, is to present an evaluation of several rubber elasticity models with respect to their ability to describe the behavior of real rubber networks. We chose the models to include a range of approaches to the development of the free energy function (related to the stress-strain response), recognizing that not all have been considered for elastic back stress calculations in the plasticity models. The intent is that, to the extent that such models correctly or incorrectly describe the behavior of real rubber networks, they may ultimately prove more or less useful in the description of the large-deformation, plastic behavior of polymers beyond the yield and in general geometries of deformation.

In the present work, we reanalyze previously published stress-strain data for rubber networks using several models. These include three broadly accepted as classical models that have been previously evaluated in different venues and three newer models that have not been evaluated as extensively, and specifically by sources other than the originators of the models. In particular, we attempt to elucidate the strengths and weaknesses of the several models that we have chosen for evaluation in light of their ability to describe the mechanical response of cross-linked rubber networks. For purposes of completeness, we also consider the predictions of the models for the deformation of swollen rubber. This recognizes the swelling as a three-dimensional isotropic deformation.

The following models are considered:

1. Phantom model [32, 33]
2. Affine model [20, 29, 47]
3. Constrained chain model [14, 15, 18, 19]
4. Localization model [9, 23, 24]
5. Liquidlike model [7, 8]
6. Eight-chain model [3].

The purpose of this paper is to compare the prediction of these models with the experimental results and to contrast the different approaches. Other models of rubber elasticity (primitive path models [10, 27], hoop model [30], reviewed by [25, 26, 31]) are not considered here.

First, we present a theoretical section in which we summarize the mechanical equations relevant to a hyperelastic material's stress-strain response. We define the Mooney-Rivlin [36, 39] framework in which we make most of our comparisons between the models and the experimental data. The important equations for swelling of rubber are then outlined, and this is followed by a brief description of the salient features of each molecular model. In particular, the strain energy density function for each is presented in a form that can be related to the mechanical and swelling equations presented in the initial paragraphs of the theoretical section.

The theoretical section is followed by a section on comparison with experimental data in which the prediction of each model is compared with the stress-strain response of both dry

and swollen rubber networks using the approach of examining the so-called reduced stress [f^*] first introduced by Mooney [36] and subsequently used by Rivlin [39] to analyze data for real networks. Finally, we make some concluding remarks.

2. THEORETICAL SECTION

2.1. Free Energy Function: Stress-Strain Response

The stress-deformation or stress-strain response of an incompressible, hyperelastic material can be written in terms of the strain energy density function, here denoted as ΔF_{el}, and the principal stretch ratios $\lambda_i, \lambda_j, \lambda_k$:

$$\sigma_i = \frac{1}{\lambda_j \lambda_k} \frac{\partial \Delta F_{el}}{\partial \lambda_i} - p, \tag{1}$$

where the subscripts refer to the principal directions of deformation, p is a hydrostatic pressure, and σ_i is the true stress in the i-direction. Also, we treat the deformation response of the rubber as incompressible so that $\lambda_1\, \lambda_2\, \lambda_3 = 1$. For uniaxial deformations such as tension and compression, the stress-strain response can be given in terms of the principal stress difference $\sigma_1 - \sigma_2$:

$$\sigma_1 - \sigma_2 = \lambda_1 \frac{\partial \Delta F_{el}}{\partial \lambda_1} - \lambda_2 \frac{\partial \Delta F_{el}}{\partial \lambda_2}. \tag{2}$$

Although it is often the case that the behavior of rubber is represented in a simple stress-deformation diagram, early in the development of both phenomenological and molecular theories of rubber elasticity, an alternative method of looking at the data arose based on the so-called Mooney-Rivlin [36, 39] representation. This powerful method of representation in terms of a reduced stress arises naturally when one examines the stress-strain relations that arise when the strain energy density function is assumed to have either a neo-Hookean form or the Mooney form.

Neo-Hookean strain energy function:

$$\Delta F_{el} = C_0 \left(\lambda_1^2 + \lambda_2^2 + \lambda_3^2 - 3\right) \tag{3}$$

Mooney-Rivlin strain energy function:

$$\Delta F_{el} = C_0 \left(\lambda_1^2 + \lambda_2^2 + \lambda_3^2 - 3\right) + C_1 \left(\lambda_1^{-2} + \lambda_2^{-2} + \lambda_3^{-2} - 3\right), \tag{4}$$

where C_i are material parameters (Mooney-Rivlin constants). The first principal stress difference $\sigma_1 - \sigma_2$ for a uniaxial deformation with $\lambda_1 = \lambda$ is then written as

$$\sigma_1 - \sigma_2 = \left(\lambda^2 - 1/\lambda\right)\left[2C_0 + 2C_1/\lambda\right], \tag{5}$$

and we can define the reduced stress $[f^*]$ by

$$[f^*] = (\sigma_1 - \sigma_2) / (\lambda^2 - 1/\lambda) = [2C_0 + 2C_1/\lambda]. \tag{6}$$

It is important to note that $[f^*]$ is a measure of the modulus of the material (in the limit of small deformations, it is the shear modulus). Hence, the Mooney-Rivlin representation, in which $[f^*]$ is plotted against $1/\lambda$, gives a much more sensitive estimate of the deviations of the material response than does the stress-deformation plot. Part of the reason stems from the fact that in a conventional stress-deformation plot, the range on the stresses runs from zero to a high value (either positive or negative). As a result, at small to intermediate deformations, deviations between experimental values of stress and those predicted by the model can be large on a relative scale (e.g., percentage error) but small in the diagram. Furthermore, part of the nonlinearity of the response of rubbery materials is a result of the large deformation geometry itself. By normalizing the stress by $(\lambda^2 - 1/\lambda)$, this is partially "corrected." Hence, for a neo-Hookean material, the plot of $[f^*]$ versus $1/\lambda$ results in a line of constant value over the entire range of deformations. For a Mooney-Rivlin material, a plot of $[f^*]$ versus $1/\lambda$ results in a straight line, with the slope and intercept at $\lambda = 1$ determining $2C_1$ and $(2C_0 + 2C_1)$, respectively. Here, we note that the phantom and affine network models discussed subsequently are neo-Hookean in form.

For emphasis, we note again that the Mooney-Rivlin representation of the data is a very sensitive tool for the evaluation of material models. This is because it is effectively a plot of the deviation of the rubbery modulus from constancy (neo-Hookean) and removes the geometrical aspects of material nonlinear behavior. This is seen by comparing Figure 1 with Figure 2. In Figure 1, we show the calculated stress-deformation behavior for a Mooney-Rivlin material as true stress versus λ along with lines that represent values 20% greater and 20% less than the model calculation. The points are deviations from the model within the region formed by the $\pm 20\%$ lines. It is clear that in the conventional stress-deformation plot, the errors are barely discernible in the region of small deformations (near to $\lambda = 1$) and appear very large as the stress magnitude increases. On the other hand, in the Mooney-Rivlin plot shown in Figure 2, the errors (dotted lines and points) are much more uniform in relative magnitude over the entire range of deformations examined, including the small deformation regime $(1/\lambda = 1)$. Hence, deviations from any given model will better manifest themselves in the Mooney-Rivlin representation than in a stress-deformation plot.

Throughout this work, most of the comparisons we make between each molecular theory and the experimental data taken from the literature for natural rubber and polydimethylsiloxane elastomer are done within the framework of the Mooney-Rivlin representation.

2.2. Free Energy Function: Swelling Response

In dealing with the elasticity of rubber networks, one important experimental procedure that has been used extensively is to swell the rubber and then deform it. Hence, because this mode of deformation brings into play important aspects of the physics of rubbery materials, we also examine the swelling behavior predicted by the molecular models considered here.

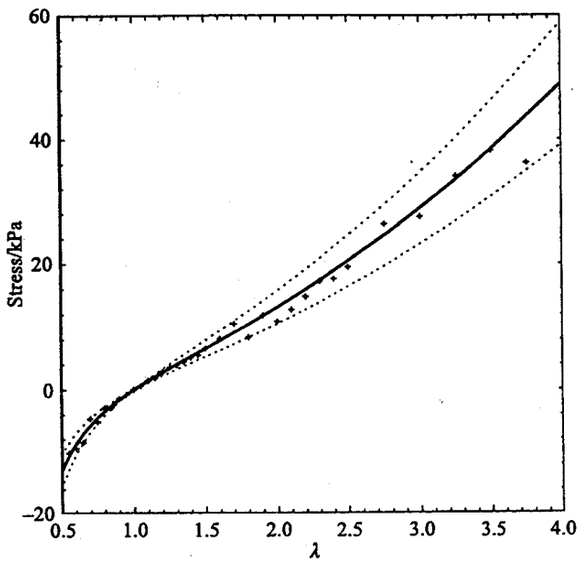

Fig. 1. Stress-deformation plot for a Mooney-Rivlin model elastomer with $C_0 = C_1 = 2.5$ kPa. Solid line depicts ideal model, dotted line represents ±20% error, and crosses are randomly generated ±20% errors.

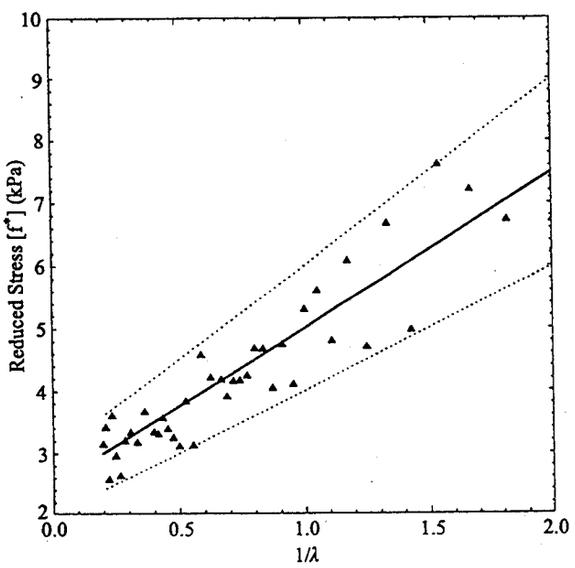

Fig. 2. Mooney-Rivlin representation of the reduced stress [f^*] versus 1/λfor the Mooney-Rivlin rubber depicted in Figure 1. Solid line is for model rubber. Points represent ±20% random error about the model. Dotted lines represent ±20% error on the model.

In the case of swelling, the models can be evaluated if we consider that the contribution to the free energy of the network due to the chain deformation is equilibrated with the contribution to the free energy due to the mixing of the solvent with the polymer. In developing the swelling theory, Frenkel [22] and Flory and Rehner [20] made the assumption that the free energy contributions due to deformation and mixing are additive and that they are described by appropriate functions for (a) the dry rubber elasticity and (b) the uncrosslinked rubber solution properties. Here, we are interested in assumption (a) that the swelling deformation behavior is described by the same function as that which describes the dry-state deformation behavior, evaluated at the appropriate values for $\lambda_s = \lambda_1 = \lambda_2 = \lambda_3$ in the case of isotropic deformations. Furthermore, we then superimpose a uniaxial mechanical deformation α on the swollen rubber. The relation between α, the total stretch (λ), and the swelling is given by

$$\lambda = \alpha (V/V_0)^{1/3} = \alpha\lambda_s, \tag{7}$$

where V_0 is the volume of the unswollen sample and V is the current swollen volume. We note that α is the deformation that refers to the swollen configuration associated with the swelling deformation $\lambda_s = (V/V_0)^{1/3}$. Substitution of the relevant deformations into the strain energy function then permits construction of the Mooney-Rivlin plot for the swollen rubber. The procedures for obtaining the general reduced stress for the swollen state are given in the appendix. The relevant equation is

$$[f^*] = \frac{(\sigma_1 - \sigma_2)}{\alpha^2 - \dfrac{1}{\alpha}} v_p^{-1/3}, \tag{8}$$

where v_p is the volume fraction of rubber. The equation is discussed in detail in the appendix (see equation (53)).

2.3. Description of the Molecular Models

The description of the molecular models follows briefly. The reader interested in more detailed analysis is referred to the cited references. For clarification of some points, there is a brief glossary of terms in the appendix.

2.3.1. PHANTOM MODEL

According to the phantom model of rubber elasticity, the polymer chains are devoid of material characteristics other than the exertion of forces on the junctions to which they are attached [32, 33]. The conformation of each chain depends only on the position of its ends and is independent of the conformations of the surrounding chains with which it shares the same region of space. The junctions in the network are free to fluctuate around their mean positions, and the magnitude of the fluctuations is strain invariant. The average positions of the junctions and of the domains of the fluctuations deform affinely with macroscopic strain. The result is that the deformation of the mean positions of the end-to-end vectors is not affine in the strain. The elastic free energy of deformation ΔF_{el} is given by

$$\frac{\Delta F_{el}}{kT} = \left(\frac{\xi}{2V_0}\right)\left(\lambda_1^2 + \lambda_2^2 + \lambda_3^2 - 3\right), \tag{9}$$

where ξ is the cycle rank of the network (see definitions in the appendix), λ_1, λ_2, and λ_3 are the principal deformation ratios, k is the Boltzmann constant, and T is absolute temperature.

Putting equation (9) for the free energy function into the constitutive (stress-strain) equation (2) and rearranging terms (equation (6)), we find the reduced stress:

$$[f^*]_{ph} = kT(\xi/V_0). \tag{10}$$

Here, we note that $[f^*]_{ph}$ is the response of a Mooney-Rivlin material in which $2C_1 = kT(\xi V_0)$ and $2C_2 = 0$; that is, a neo-Hookean material. Note that it is independent of deformation.

Following the procedure detailed in the appendix, we obtain the following first principal stress difference in the swollen state:

$$\sigma_1 - \sigma_2 = \nu_p \lambda_s^2 \left(\frac{\xi kT}{2V_0}\right)\left(2\alpha_1^2 - 2\alpha_2^2\right) = 2\nu_p^{1/3}\left(\frac{\xi kT}{2V_0}\right)\left(\alpha_1^2 - \alpha_1^{-1}\right). \tag{11}$$

Since we use the following definition of the reduced stress $[f^*]$ for the swollen rubber,

$$[f^*] = \nu_p^{-1/3}\frac{(\sigma_1 - \sigma_2)}{\alpha_1^2 - \alpha_1^{-1}}, \tag{12}$$

the reduced stress for the neo-Hookean type models does not have any swelling dependence as shown in the following equation:

$$[f^*] = \frac{\xi kT}{V_0}. \tag{13}$$

2.3.2. AFFINE MODEL

In the affine model [20, 29, 47], it is assumed that the displacement of the mean positions of the junctions should transform linearly in the macroscopic strain (affine deformation) and, hence, that the transformation of the distribution of the end-to-end vectors of the chains should likewise be affine. Fluctuations of the network junctions are completely suppressed by intermolecular interactions with neighboring coils sharing the same region of space. The elastic free energy is given by

$$\frac{\Delta F_{el}}{kT} = (\nu_{el}/2V_0)\left(\lambda_1^2 + \lambda_2^2 + \lambda_3^2 - 3\right) - (\mu_{el}/V_0)\ln(\lambda_1\lambda_2\lambda_3), \tag{14}$$

where ν_{el} and μ_{el} are the number of elastic chains and junctions, respectively.

The reduced stress is then written as

$$[f^*]_{aff} = kT(\nu_{el}/V_0), \tag{15}$$

and again we have a neo-Hookean response. Therefore, the reduced stress in the swollen state is the same as in the dry state.

We note that in both the phantom and affine models, the reduced stress is independent of stretch ratio, but their numerical values are different. For a perfect tetra functional network (see above references), $\xi = \nu_{el}/2$; that is, $[f^*]_{ph} = [f^*]_{aff}/2$.

2.3.3. CONSTRAINED CHAIN MODEL

In real networks, intermolecular entanglements and other steric (geometrically caused) constraints on the fluctuations of junctions also contribute to the elastic free energy. To describe the experimentally observed deviations from ideal elastic behavior, Ronca and Allegra [41] and Flory [18] introduced the assumptions of constrained fluctuations of the junctions and of affine deformations of the fluctuation domains.

In the constrained junction fluctuation model developed by [18] and Flory and Erman [19], the conformational constraints are assumed to act solely on the network junctions. The size of the domains of constraint is assumed to decrease with increasing strain so that the junction fluctuations become larger. The most important new parameter in this model is κ, the measure of the severity of the constraints relative to those imposed by a phantom network,

$$\kappa = < \Delta R^2 >_{ph} / < \Delta s^2 >_0, \tag{16}$$

where $< \Delta R^2 >_{ph}$ is the mean squared fluctuation of junctions in the phantom network model and $< \Delta s^2 >_0$ is the mean squared fluctuation of junctions in the constrained network model. In the phantom model, there are no constraints; consequently, $\kappa = 0$. If the constraints are infinitely strong, $< \Delta s^2 >_0$ is zero and κ goes to infinity (affine model).

The elastic free energy is given by

$$\Delta F_{el} = \Delta F_{el}^{ph} + \Delta F_{el}^{c}, \tag{17}$$

where ΔF_{el}^{c} is the contribution arising from entanglement constraints relative to those in the phantom network. This term can be written

$$\frac{\Delta F_{el}^{c}}{kT} = \left(\frac{\mu_{el}}{2V_0}\right) \sum_{i=1}^{3} \left[(1+g_i) B_i - \ln\left((B_i+1)(g_i B_i+1)\right)\right], \tag{18}$$

with

$$B_i = (\lambda_i - 1)\left(1 + \lambda_i - \zeta \lambda_i^2\right)(1+g_i)^{-2} \tag{19a}$$

$$g_i = \lambda_i^2 \left[\kappa^{-1} + \zeta\,(\lambda_i - 1)\right], \tag{19b}$$

where the parameter ζ characterizes the nonaffine transformation of the domains of constraints with deformation.

The constrained junction fluctuation theory was refined by [14]. The fundamental difference between the new constrained chain model and the original theory is the adoption

of the more realistic assumption that the constraints affect the whole chain rather than the cross-links only. Initially, the original Flory-Erman model and the Erman-Monnerie model were easily related. However, in 1992 Erman and Monnerie [15] published corrections to the model, which we use in the following paragraphs.

Instead of using the two parameters κ and ζ in addition to the network properties, to fit the stress-strain swelling data, the new theory uses a single parameter κ_G, which appears in the following equation:

$$h(\lambda_i) = \kappa_G \left[1 + \frac{(\lambda_i^2 - 1)\left(1 - \frac{2}{f}\right)^{2/3}}{3} \right], \tag{20}$$

where f is the functionality of the network junction (see the glossary in the appendix).

We refer to equation (17) for the free energy, where ΔF_{el}^{ph} is the phantom contribution given previously and, now, ΔF_{el}^{c} is the contribution arising from the constraint effects and is given as follows:

$$\Delta F_{el}^{c} = \frac{1}{2}\xi kT \sum_i \left(\lambda_i^2 - 1 + (\nu_{el}/\xi)\left[B_i + D_i - \ln(1 + B_i) - \ln(1 + D_i)\right]\right) \tag{21}$$

$$B_i = \frac{h(\lambda_i)\,\kappa_G \left(1 - \left(1 - \frac{2}{f}\right)^{2/3}\right)(\lambda_i^2 - 1)}{\left[\lambda_i^2 + h(\lambda_i)\right]^2} \qquad D_i = \frac{\lambda_i^2 B_i}{h(\lambda_i)}. \tag{22}$$

Then, the reduced stress $[f^*]$ in the dry state is given by [14, 15]

$$[f^*] = [kT\xi/V_0]\,(1 + f_c/f_{ph}) = [f^*]_{ph}\,(1 + f_c/f_{ph}), \tag{23}$$

and, in the swollen state,

$$[f^*] = [f^*]_{ph}\,[1 + (\nu_{el}/\xi)]\left[\alpha K(\lambda_x^2) - \alpha^{-2} K(\lambda_y^2)\right] \frac{1}{(\alpha - \alpha^{-2})}, \tag{24a}$$

where

$$K(\lambda_i^2) = \frac{B_i \dot{B}_i}{(1 + B_i)} + \frac{D_i \dot{D}_i}{1 + D_i} \tag{24b}$$

$$\dot{B}_i = B_i \left(\frac{1}{(\lambda_i^2 - 1)} - \frac{2}{\left[\lambda_i^2 + h(\lambda_i)\right]} + \frac{\kappa_G \left[\lambda_i^2 - h(\lambda_i)\right]\left(1 - \frac{2}{f}\right)^{2/3}}{h(\lambda_i)\left[\lambda_i^2 + h(\lambda_i)\right]} \right) \tag{25}$$

and

$$\dot{D}_i = B_i \left[h(\lambda_i)^{-1} - \frac{\lambda_i^2 \kappa_G \left(1 - \frac{2}{f}\right)^{2/3}}{h(\lambda_i)^2} \right] + \frac{\lambda_i^2 \dot{B}_i}{h(\lambda_i)}. \tag{26}$$

Importantly, this model is not Mooney-Rivlin in its response, since the compression behavior bends over to a nearly constant value, as observed experimentally and discussed later. Also, it was pointed out by McKenna and Hinkley [35] that for the original Flory-Erman model, $d\Delta F_{el}/d\lambda|_{\lambda-1} > 0$, which may lead to thermodynamic stability problems [e.g., 6, 43], but this is not of concern here.

2.3.4. LOCALIZATION MODEL

Gaylord and Douglas [23, 24] incorporated into a simple theory the minimal features of rubber networks: the connectivity of the chain segments on a global scale, the entanglement interactions on a local scale, and the finite volume of the chains. The elastic free energy is given as the sum of two terms: one is proportional to the cross-link density and has the same form as the phantom network, the other accounts for the loss of degrees of freedom of the chains due to chain localization. The chains are localized in a tube defined by the interactions with neighboring chains. In a dry rubber, the radius of the tube reflects the hard-core cross-sectional radius of the polymer, and the volume of the tube is comparable with the molecular volume of the chain. The tube volume is considered to be invariant with macroscopic strain, since the molecular volume of the chains is independent of the deformation. On the basis of this assumption, the variation of the chain localization length with the extent of deformation ratio is calculated. The elastic free energy of the network is given by

$$\Delta F_{el} = (G_v/2)\left(\lambda_1^2 + \lambda_2^2 + \lambda_3^2 - 3\right) + G_e\left(\lambda_1 + \lambda_2 + \lambda_3 - 3\right), \tag{27}$$

where

$$G_v = \frac{\nu_{el} kT}{2V_0} \tag{28}$$

and

$$G_e = \gamma G_v + G_N. \tag{29}$$

G_N is the plateau modulus of the polymer melt, and γ is a constant. In the absence of localization interactions, $G_e = 0$, and equation (23) reduces to the result obtained for the phantom model.

This theory yields for the reduced stress

$$[f^*] = G_v + G_e\left(1 - \lambda^{-3/2}\right)/\left(\lambda - \lambda^{-2}\right). \tag{30}$$

The localization model shows a swelling dependent reduced stress. The first principal stress difference is given by

$$\begin{aligned}\sigma_1 - \sigma_2 &= \nu_p \left(\frac{G_v}{2} \lambda_s^2 2\alpha_1^2 - \frac{G_v}{2} \lambda_s^2 2\alpha_2^2 + G_e \lambda_s \alpha_1 - G_e \lambda_s \alpha_2 \right) \\ &= \nu_p^{1/3} G_v \left(\alpha_1^2 - \alpha_1^{-1} \right) + \nu_p^{2/3} G_e \left(\alpha_1 - \frac{1}{\sqrt{\alpha_1}} \right) \\ &= \nu_p^{1/3} \left(\alpha_1^2 - \alpha_1^{-1} \right) \left(G_v + \nu_p^{1/3} \frac{\left(1 - \alpha_1^{-3/2} \right)}{\left(\alpha_1 - \alpha_1^{-2} \right)} \right). \end{aligned} \tag{31}$$

Then, the reduced stress in the swollen state [9] for the localization model is given as follows:

$$[f^*] = G_v + \nu_p^{1/3} G_e \frac{\left(1 - \alpha_1^{-3/2} \right)}{\left(\alpha_1 - \alpha_1^{-2} \right)}. \tag{32}$$

Treatment of the swelling problem with this model may require an estimation of the change of G_e with dilution [9]. Here, we treat it as a constant.

2.3.5. LIQUIDLIKE MODEL OF RUBBER ELASTICITY

The liquidlike model developed by DiMarzio [7, 8] accounts for the orientation dependent packing entropy that reduces the force when the network is stretched. It is argued that chain entanglements result in an increase in the effective number of chain segments when the chain is stressed. The configurational constraints arising from entanglements are modeled by a slip ring. The slip ring and the end points of the chains move affinely with macroscopic strain. When the slip ring moves, the segments in each of the two parts of the chain separated by the slip ring adjust themselves to minimize the free energy. This leads to an extra term in addition to the elastic free energy term of the phantom model:

$$\Delta F_{el}/kT = A_1 \left(\lambda_1^2 + \lambda_2^2 + \lambda_3^2 - 3 \right) + A_2 \left(\lambda_1 \lambda_2 + \lambda_2 \lambda_3 + \lambda_3 \lambda_1 - 3 \right), \tag{33}$$

where A_1 and A_2 are constants. Here, $A_1 = \nu_{el}/2V_0$ and A_2 is proportional to kT and the number of chains per unit volume. The rearrangement of the chains leads to an apparent increase in the number of chain segments as the chain is stretched. Since the conformational entropy of the chains, which is responsible for the equilibrium force in a Gaussian network, always decreases upon deformation, this model gives a correction to the force that is of the opposite sign; that is, as the chains are stretched, the equilibrium forces become smaller.

The reduced stress is given by

$$[f^*]/kT = 2A_1 + A_2 \left(\lambda^{-1/2} - \lambda^{-2} \right) / \left(\lambda - \lambda^{-2} \right). \tag{34}$$

Although it is not neo-Hookean, the liquidlike model gives a reduced stress that does not depend on swelling. The free energy in the swollen state is given as follows:

$$\begin{aligned}\Delta F_{el,s} &= \nu_p \Delta F_{el,d} = \nu_p kT\left(A_1\left(\lambda_s^2\left(\alpha_1^2+\alpha_2^2+\alpha_3^3\right)-3\right)\right.\\ &\left.+A_2\left(\lambda_2^2\left(\alpha_1\alpha_2+\alpha_2\alpha_3+\alpha_3\alpha_1\right)-3\right)\right).\end{aligned} \tag{35}$$

Subsequently, the principal stress difference can be readily shown as follows:

$$\sigma_1-\sigma_2=\nu_p^{1/3}kT\left(2A_1\left(\alpha_1^2-\alpha_1^{-1}+A_2\left(\alpha_1\frac{2}{\sqrt{\alpha_1}}-\frac{1}{\sqrt{\alpha_1}}\left(\alpha_1+\frac{1}{\sqrt{\alpha_1}}\right)\right)\right)\right). \tag{36}$$

Therefore, the reduced stress in the swollen state is given by

$$[f^*]=\frac{(\sigma_1-\sigma_2)\,\nu_p^{-\frac{1}{3}}}{(\alpha^2-\alpha^{-1})}=kT\left(2A_1+A_2\frac{\left(\alpha^{-\frac{1}{2}}-\alpha^{-2}\right)}{\alpha-\alpha^{-2}}\right), \tag{37}$$

and this is clearly independent of the amount of swelling.

2.3.6. EIGHT-CHAIN MODEL

This constitutive model, developed by Arruda and Boyce [3], is based on an eight-chain representation of the molecular network structure of the rubber and the non-Gaussian behavior of the chains. The model describes the cooperative nature of network deformation and requires two material parameters: the initial modulus and the limiting chain extensibility; that is, the fact that the network chains have a finite length between cross-link points and, therefore, cannot be extended to an infinite extent. The finite extensibility is accounted for by using the inverse Langevin expression for the chain entropy. This approach was first suggested by Wang and Guth [48] and developed more fully by Treloar [44]. In the eight-chain model, the chain extension is reduced to a function of the root mean square of the principal applied stretches as a result of effectively sampling eight orientations of principal stretch space. The eight-chain model is formulated such that the network chains reach the individual chain extensibility limit at different imposed global stretch levels. The free energy of the network is written as

$$\Delta F_{el}=\frac{\nu_{el}}{V_0}kTN\left(\frac{\beta}{\sqrt{N}}\lambda_{chain}+\ln\frac{\beta}{\sinh(\beta)}\right)-TC, \tag{38}$$

where T is absolute temperature, $\beta=\mathcal{L}^{-1}\left[\lambda_{chain}/\sqrt{N}\right]$ and $\mathcal{L}^{-1}$ is the inverse Langevin function, λ_{chain} is the chain stretch, N is the number of segments between two nearest neighboring cross-links, and C is a constant. λ_{chain} is related to the macroscopic deformations through the first stretch invariant, I_1:

$$\lambda_{chain} = \frac{I_1^{1/2}}{\sqrt{3}} = \frac{(\lambda_1^2 + \lambda_2^2 + \lambda_3^2)^{1/2}}{\sqrt{3}}. \tag{39}$$

The Langevin function is defined as

$$\mathcal{L}(t) = \coth(t) - \frac{1}{t}. \tag{40}$$

The series expansion of the inverse Langevin function gives [44]

$$\mathcal{L}^{-1}[t] = 3t + \frac{9}{5}t^3 + \frac{297}{175}t^5 + \frac{1539}{875}t^7 + \frac{126117}{67375}t^9 + \ldots, \tag{41}$$

where $t = \lambda_{chain}/\sqrt{N}$. Since the convergence of the above series expansion deteriorates as the argument t increases, we numerically solve the inverse Langevin function using the Newton-Raphson method for large t in our solutions to the eight-chain model.

From equations (2) and (6) (the latter giving the definition of $[f^*]$), the reduced stress for the eight-chain model in the dry state can be readily shown to be

$$[f^*] = \frac{(\sigma_1 - \sigma_2)}{\lambda_1^2 - 1/\lambda_1} = \frac{\nu_{el}}{3V_0}\frac{kT\sqrt{N}}{\lambda_{chain}}\mathcal{L}^{-1}\left[\frac{\left(\lambda_1^2 + \frac{2}{\lambda_1}\right)^{1/2}}{\sqrt{3N}}\right]. \tag{42}$$

The effect of swelling can be taken into account in the eight-chain model by evaluating the free energy function in the swollen state at values of the stretch appropriate to the combination of the swelling stretch $\lambda_s = \nu_p^{-1/3}$ and the superimposed mechanical deformations α_i. Also, we note that ν_p is the volume fraction of the polymer in the swollen system. Then, the strain energy contribution to the free energy of the swollen rubber becomes

$$\Delta F_{el,s} = \nu_p \frac{\nu_{el}}{V_0} kTN \left(\frac{\nu_p^{-1/3}\lambda^*_{chain}}{\sqrt{N}}\mathcal{L}^{-1}\left[\frac{\nu_p^{-1/3}\lambda^*_{chain}}{\sqrt{N}}\right] + \ln\left[\frac{\mathcal{L}^{-1}\left[\frac{\nu_p^{-1/3}\lambda^*_{chain}}{\sqrt{N}}\right]}{\sinh \mathcal{L}^{-1}\left[\frac{\nu_p^{-1/3}\lambda^*_{chain}}{\sqrt{N}}\right]}\right]\right) - TC, \tag{43}$$

and we define λ^*_{chain} in terms of the mechanical deformations α_i:

$$\lambda^*_{chain} = \frac{(\alpha_1^2 + \alpha_2^2 + \alpha_3^2)^{1/2}}{\sqrt{3}}. \tag{44}$$

Using the procedure given in the appendix, we obtain the following reduced-stress equation from the eight-chain model for the swollen rubber:

$$[f^*] = \frac{(\sigma_1 - \sigma_2)\, \nu_p^{-1/3}}{\alpha_1^2 - 1/\alpha_1} = \frac{\nu_{el}}{3V_0} kT\sqrt{N} \frac{\nu_p^{1/3}}{\lambda^*_{chain}} \mathcal{L}^{-1}\left[\frac{\nu_p^{-1/3}\left(\alpha_1^2 + \frac{2}{\alpha_1}\right)^{1/2}}{\sqrt{3N}}\right]. \quad (45)$$

3. RESULTS

3.1. Stress-Strain Response of Dry Rubber Networks

In the introduction, we discussed qualitatively the concept of using a Mooney-Rivlin plot to analyze the models discussed above as the context for comparing them with literature data for the stress-strain response of natural rubber (NR) and a polydimethylsiloxane (PDMS) rubber. In Figure 3a, we depict typical stress-deformation plots for both rubber types. Figure 3b depicts the corresponding Mooney-Rivlin plot in which the reduced stress is plotted against the reciprocal of the stretch λ. One sees immediately that the Mooney-Rivlin plot distinguishes between the two rubbers over the entire range of data, whereas the stress-deformation plot does so only at the large deformations. In the following paragraphs, we first present qualitative features of the rubber elasticity models discussed above. We then compare model calculations with the data of Figures 3a and 3b in a quantitative fashion.

3.2. Qualitative Features of the Rubber Models: Dry State

In this section, we present a qualitative comparison of the stress-strain behaviors given by the different models for dry rubber. We are particularly interested in the models that yield similar dependencies and those that give divergent results.

In Figures 4a and 4b, we depict the responses for the models, along with that of the Mooney-Rivlin model, in the reduced-stress or Mooney-Rivlin plot. The parameters were chosen to give similar moduli in the small strain region. The parameters used for each model are presented in Table 1. If we look first to Figure 4a, we note that the value of $[f^*]$ is constant for both the phantom and affine network models; the Mooney-Rivlin material gives a straight line over the whole range of deformations. Recalling Figure 3b, these are not even qualitatively correct behaviors for the reduced stress. On the other hand, both the localization and liquidlike models exhibit qualitatively correct behavior; that is, an increasing value of $[f^*]$ as $1/\lambda$ increases (on the tension side of $1/\lambda$) followed by a significant curvature as one goes into compression ($1/\lambda > 1$). Examination of Figure 4b shows again the phantom, affine, and Mooney-Rivlin models, as well as the constrained chain and eight-chain models. The constrained chain model exhibits qualitatively correct behavior (i.e., decreasing value of $[f^*]$ as tensile stress increases and a curvature and mild decrease in $[f^*]$ as one goes through zero deformation ($1/\lambda = 1$) and into compression). On the other hand, the eight-chain model exhibits nonqualitative behavior, since it shows a dramatic increase in $[f^*]$ in tension and a gently increasing value of $[f^*]$ as the deformation goes into compression. The dramatic

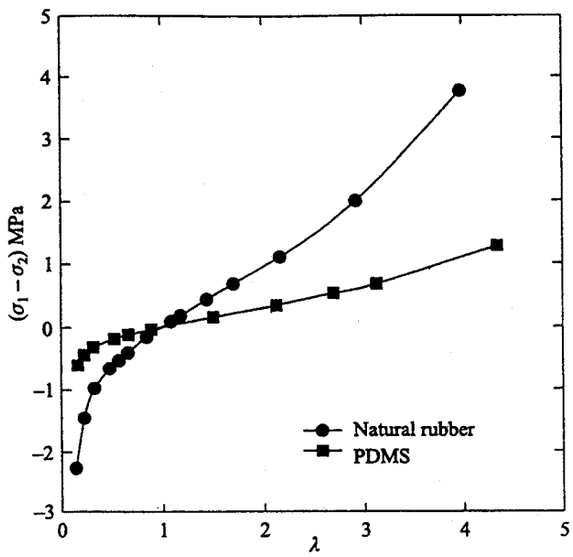

Fig. 3a. True stress-deformation plot for unswollen natural rubber and polydimethylsiloxane (PDMS) elastomer. Natural rubber data are from Rivlin and Saunders [40], and PDMS data are from Pak and Flory [38].

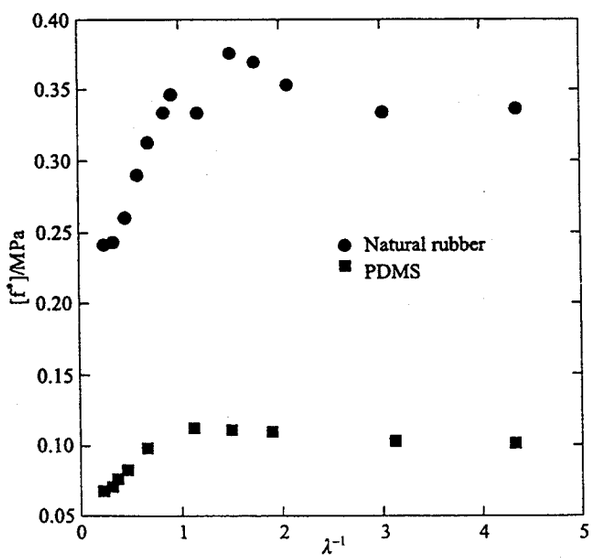

Fig. 3b. Reduced stress versus reciprocal deformation (Mooney-Rivlin) representation of the stress-deformation behavior of natural rubber and polydimethylsiloxane (PDMS) elastomer. Natural rubber data are from Rivlin and Saunders [40], and PDMS data are from Pak and Flory [38].

Table 1. Model parameters used in calculations for unswollen rubber used to construct Figures 4a and 4b

Model	*Parameter*	*Value*
Phantom	$[f^*]_{ph}$ /MPa	0.06
Affine	$[f^*]_{aff}$ /MPa	0.12
Mooney-Rivlin	C_0/MPa	0.03
	C_1/MPa	0.01
Constrained chain	κ_G	3.58
	$[f^*]_{ph}$ /MPa	0.06296
Eight-chain	N	100
	$\nu kTV_0^{-1}/MPa$	0.098
Localization	G_ν/MPa	0.0356
	G_e/MPa	0.1449
Liquid like	A_1kT/MPa	0.0367
	A_2kT/MPa	0.0402

increase in $[f^*]$ (or nonlinear modulus) undoubtedly is due to the fact that the eight-chain model invokes immediately limited chain extensibility. Hence, one gets "hardening" upon deformation of the network as exhibited by the rapid increase in $[f^*]$ with increasing tension (decreasing $[f^*]$). Hence, one could say that the eight-chain model suffers from the same type of inadequacies as does the Mooney-Rivlin model, except the Mooney-Rivlin hardens in compression while the eight-chain model shows hardening in tension. The observed minimum in the reduced stress for the eight-chain model is surprising, particularly the upturn that occurs immediately in tension $(1/\lambda < 1)$. This phenomenon has never been observed experimentally, to our knowledge, in unfilled rubber. In fact, much early work in rubber elasticity sought to explain why the reduced stress $[f^*]$ decreases as $1/\lambda$ decreases (tension) rather than remaining constant as in the phantom and affine models, and as represented by the Mooney-Rivlin model in the figure.

The following sentences provide some detailed remarks about Figures 4a and 4b. According to the phantom and affine models, $[f^*]$ is independent of λ^{-1} (neo-Hookean models). The constrained chain model predicts an intermediate behavior between the phantom and the affine models. At deformations close to $\lambda^{-1} = 1$, $[f^*]$ is close to the prediction of the affine model (upper horizontal straight line). $[f^*]$ decreases with increasing deformation (decreasing λ^{-1}) and approaches that of the phantom network (lower horizontal straight line). The localization model predicts behavior of $[f^*]$ with λ^{-1} that is a qualitatively similar to that of the constrained chain model. In extension $(\lambda^{-1} < 1)$, the prediction of the liquidlike model is between that of the constrained chain model and the localization model. In the compression range $(\lambda^{-1} > 1)$, however, the two models differ significantly. The liquidlike model does not predict a maximum in the $[f^*]$ versus λ^{-1} curve; rather, it continues to increase monotonically with increasing λ^{-1}. It is also clear from this figure that the eight-chain model produces an upswing in $[f^*]$ with increasing deformation in both extension and compression. This is due to the implementation in the model of the inverse Langevin function to account for the finite extensibility of the network chains. As mentioned above and shown later, this is an unphysical response.

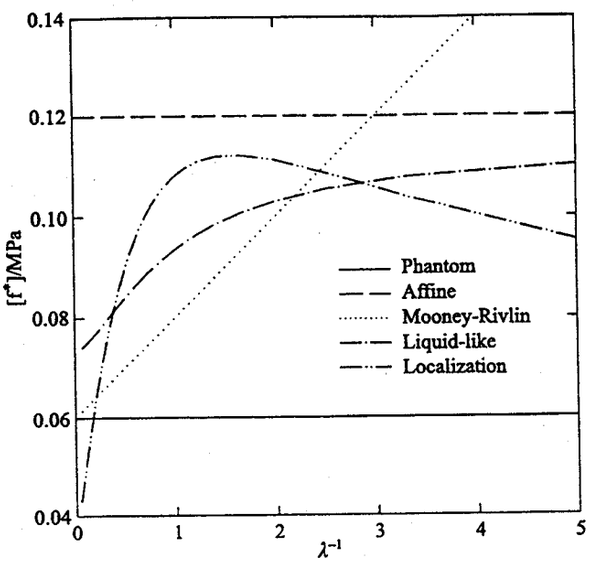

Fig. 4a. Mooney-Rivlin representation of stress-deformation responses for several rubber models.

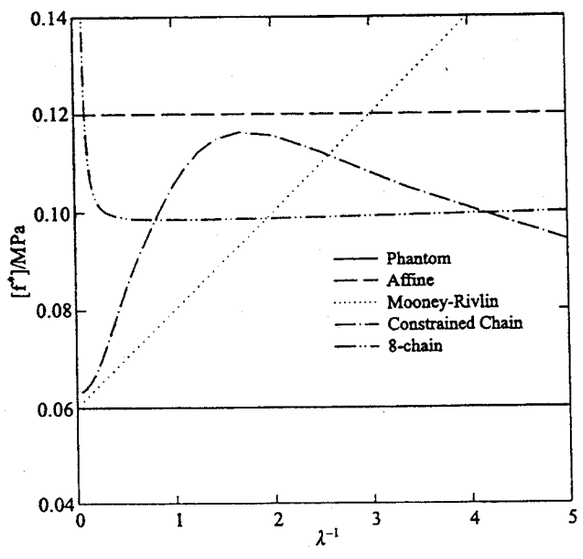

Fig. 4b. Mooney-Rivlin representation of stress-deformation responses for several rubber models.

Table 2. Model parameters used to calculate stress-deformation behavior of unswollen natural rubber and polydimethylsiloxane elastomer data relevant to Figures 5a and 5b

Material		*Natural Rubber*	*Polydimethylsiloxane*
Constrained	κ_G	2.879	3.58
chain model	$[f^*]_{ph}$ /MPa	0.2137	0.06296
Localization	G_v/MPa	0.1377	0.0356
model	G_e/MPa	0.4183	0.1449
Liquid like	A_1kT/MPa	0.1271	0.0367
model	A_2kT/MPa	0.1201	0.0402
Eight-chain	N	100	100
model	νkTV_0^{-1}/MPa	0.35	0.098

3.6.1. COMPARISON OF RUBBER MODELS WITH DRY RUBBER DEFORMATION DATA

In these paragraphs, we discuss the quantitative comparison between the rubber models chosen for evaluation and the experimental data presented in Figures 3a and 3b. In each case, we attempted to optimize the fit of the models to the data. The appropriate parameters are shown in Table 2. In Figure 5a, we depict the natural rubber data along with comparisons with the fits from the constrained chain model, the localization model, the liquidlike model, and the eight-chain model. We do not present the results for the phantom, affine, or Mooney-Rivlin models, since they are known not to fit such data. In Figure 5b, we show a similar plot for the PDMS rubber. It is clear from Figures 5a and 5b that only the constrained chain and the localization models capture the full range of behaviors for both rubbers. Although the liquidlike model is reasonable, it does not capture the maximum in $[f^*]$ at values of $1/\lambda$ approaching unity. The eight-chain model is not even qualitatively correct. It exhibits a strong increase in $[f^*]$ in tension, goes through a minimum near to zero deformation, and then increases again as one goes into compression. The actual data clearly show a maximum in $[f^*]$ in going from tension to compression and slightly offset from zero deformation toward $1/\lambda$ in the vicinity of 1.5.

3.6.2. QUALITATIVE FEATURES OF THE RUBBER MODELS: SWOLLEN STATE

As noted previously, swelling provides a three-dimensional deformation of the molecular chains and, as a result, is a severe test of the molecular models. Although parts of swelling theory are still not completely satisfactory, it is still possible to compare the behavior of the molecular models with the behavior observed in real rubber networks. In Figures 6a and 6b, the effects of swelling on the theoretical $[f^*]$ versus α^{-1} dependencies are compared for the different models. In Figure 6a, we have depicted the reduced stress versus inverse deformation curves for the affine, phantom, and Mooney-Rivlin models, as well as the localization and constrained chain models, for networks in the dry ($\nu_p = 1.0$) and increasingly swollen ($\nu_p = 0.75; \nu_p = 0.50$) states. Importantly, in this reduced-stress representation, the affine and phantom models indicate no change in the reduced stress upon swelling. In general, any strain energy functions having only terms of the same polynomial

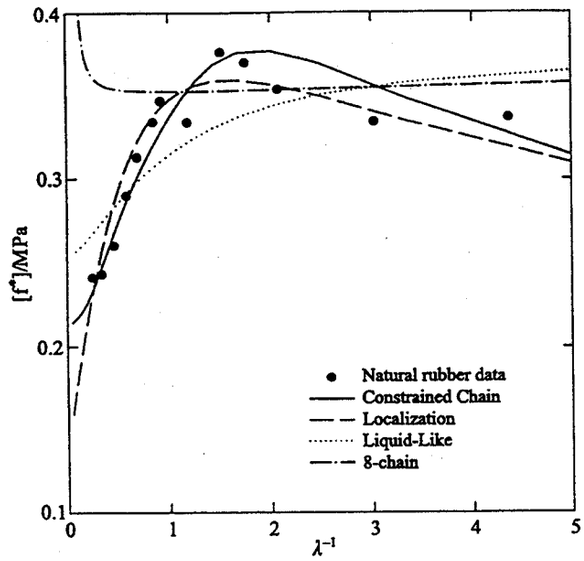

Fig. 5a. Comparison of model calculations for reduced stress with natural rubber data of Rivlin and Saunders [40]. Points are data, and lines are models.

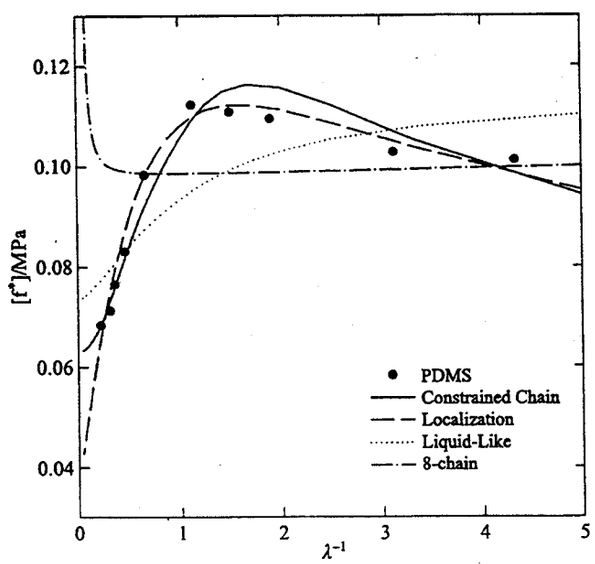

Fig. 5b. Comparison of model calculations for reduced stress with polydimethylsiloxane (PDMS) elastomer data of Pak and Flory [38]. Points are data, and lines are models.

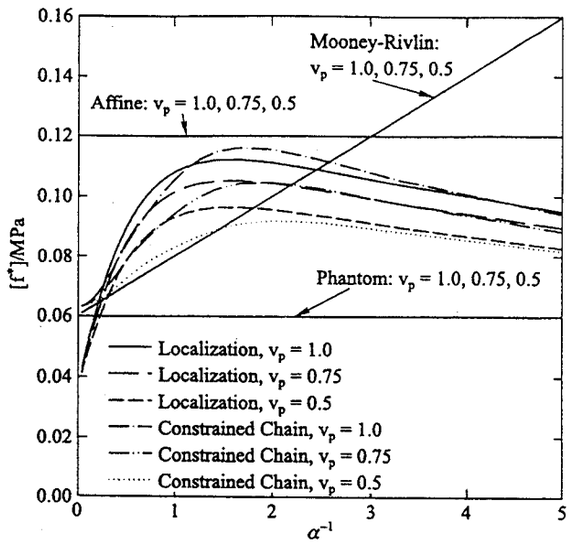

Fig. 6a. Mooney-Rivlin representation of stress-deformation response for swollen rubber as calculated using models discussed in text.

orders of stretch ratio product will give rise to the same behavior (see the appendix). This observation is in agreement with experimental observation [1] and is shown later.

In Figure 6b, we give a Mooney-Rivlin representation of the stress-deformation behavior of the liquidlike and eight-chain models, as well as the affine, phantom, and Mooney-Rivlin models (see equation (55) in the appendix). The results show that the phantom, affine, and liquidlike models give reduced stresses that are independent of the degree of swelling. The Mooney-Rivlin and eight-chain models show a decrease in reduced stress as the degree of swelling increases. Although the Mooney-Rivlin model shows an unphysical linear increase in the reduced stress when going from extension to compression and beyond, a simple empirical variation of the Mooney-Rivlin model has been known to fit weak extension-strain behavior of some swollen natural rubber using dry-state parameters only [37]. Although the reduced stress (see the appendix) for the Mooney-Rivlin model could fit the extension data in the weakly stretched swollen state rather nicely, we do not attempt to use the Mooney-Rivlin model further because of its unphysical prediction for the rubber behavior in compression. The eight-chain model shows the effects of swelling on the limited chain extensibility as a shift in the upturn point of the curve to lower values of stretch as the degree of swelling increases. Swelling does not change the qualitative shape of the curve; its unphysical feature remains unchanged.

3.6.3. COMPARISON OF RUBBER MODELS WITH SWOLLEN RUBBER DEFORMATION DATA

Figure 7a gives a plot of $[f^*]$ versus α^{-1} for natural rubber in the dry and swollen states. The data show dramatically the impact of swelling on the mechanical response of the rubber. It

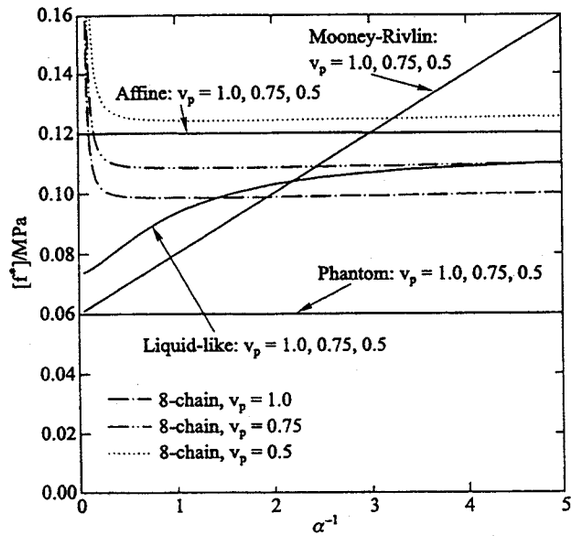

Fig. 6b. Mooney-Rivlin representation of stress-deformation response for swollen rubber as calculated using models discussed in text.

is clear that as the material swells, the reduced stress at small deformations becomes smaller while the behaviors at larger deformations (smaller values of α^{-1}) seem to merge. Similar data are depicted for a PDMS rubber in Figure 7b. Because the only models that show, even qualitatively, the reduction in reduced stress upon swelling are the constrained chain and the localization models, we consider only these in the following direct comparison with the data. It is worth emphasizing at this stage that the affine, phantom, and liquidlike models all fail because they do not capture the decrease in $[f^*]$ as the degree of swelling increases. The Mooney-Rivlin and eight-chain models show a decreasing reduced stress with increasing degree of swelling. However, Mooney-Rivlin gives a continuing linear increase when going from extension to compression, and the eight-chain model does not change its unphysical stretch-stress behavior when swelling is considered.

In Figure 8a, the comparison between the NR data and the localization and constrained chain models is shown for unswollen ($\nu_p = 1.0$) and swollen ($\nu_p = 0.61; \nu_p = 0.36$) rubber. A similar comparison is made for the PDMS rubber and the two models in Figure 8b for unswollen ($\nu_p = 1.0$) and swollen ($\nu_p = 0.85; \nu_p = 0.61; \nu_p = 0.46$) rubber. The parameters used for the curves are given in Table 3. Although both models capture the data reasonably well, the constrained chain model seems to give a qualitatively better agreement with the data. More interesting is the observation that the constrained chain model seems to have an asymptotic limit of $\alpha^{-1} \rightarrow 0$, whereas such is not the case with the localization model. This suggests the need for experiments in which the rubber can be deformed to larger extensions in the swollen state—a task that may be impossible due to the friability of swollen networks. Furthermore, the value of G_ν becomes negative for the swollen PDMS in the localization model. This is unphysical and may require consideration of the swelling dependence of G_e as indicated previously. This is beyond the scope of the current work.

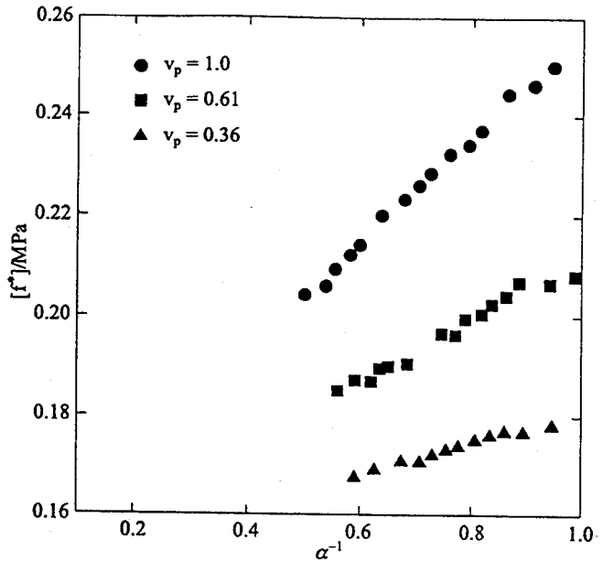

Fig. 7a. Mooney-Rivlin representation of the reduced stress for swollen natural rubber. Data are from Allen et al. [1] for different volume fractions of rubber v_p.

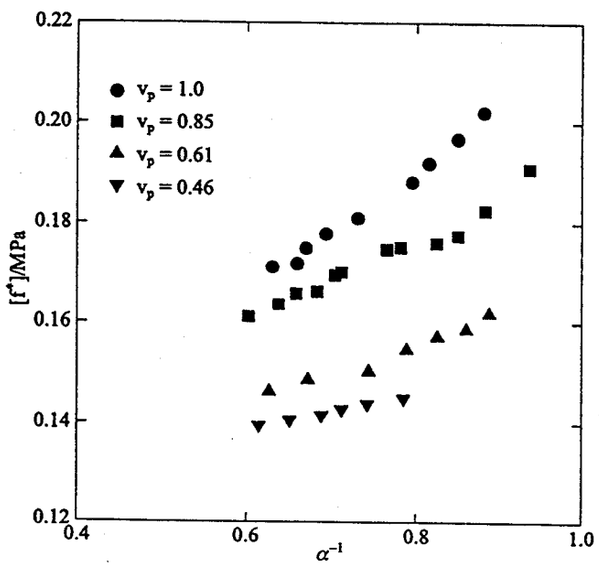

Fig. 7b. Mooney-Rivlin representation of the reduced stress for swollen polydimethylsiloxane (PDMS) elastomer. Data are from Flory and Tatara [21] for different volume fractions of rubber v_p.

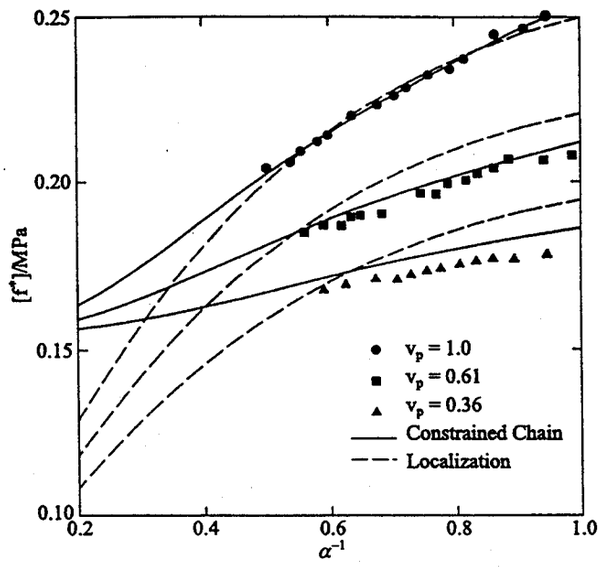

Fig. 8a. Comparison of constrained chain and localization model calculations with reduced-stress data for swollen natural rubber. Points are data from Allen et al. [1] for different volume fractions of rubber v_p, and lines are model calculations.

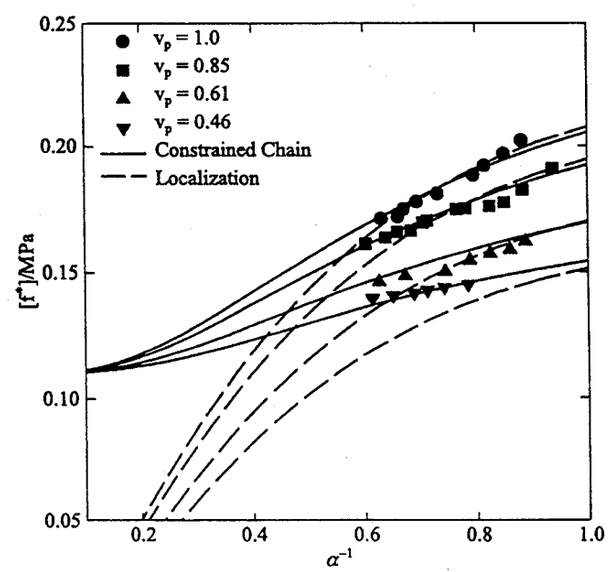

Fig. 8b. Comparison of constrained chain and localization model calculations with reduced-stress data for swollen polydimethylsiloxane (PDMS) elastomer. Points are data from Flory and Tatara [21] for different volume fractions of rubber v_p, and lines are model calculations.

Table 3. Parameters used in Figures 8a and 8b for constrained chain and localization model calculations of swollen state behavior for natural rubber and polydimethylsiloxame elastomer

Network/Solvent		*Natural Rubber/* n-*decane*	*Polydimethylsiloxane/ benzene*
Constrained	κ_G	3.441	5.404
chain model	$[f^*]_{ph}$ /MPa	0.1534	0.1093
Localization	G_v /MPa	0.059	−0.0385
model	G_e/MPa	0.3815	0.4927

4. CONCLUSIONS

The purpose of this paper is to examine several models of rubber elasticity and their ability to describe the experimentally observed behavior of rubber networks in both dry and swollen states. We evaluated (and used as a sort of baseline) the classical affine and phantom models, as well as the phenomenological Mooney-Rivlin model. In addition, the constrained chain model of [14, 15], the localization model of [23, 24], the eight-chain model of [3], and the liquidlike model of [8] were evaluated. There are several important results. First, we showed that the Mooney-Rivlin representation of reduced stress versus reciprocal of the stretch is a very sensitive measure of deviations of actual behavior from those predicted by different models (or ideal) over the entire range of deformations from very small to very large. Along with this point, it was demonstrated that simple stress-elongation curves emphasize the behavior at large deformations and hide discrepancies between model and data in the small-to-intermediate deformation range.

Second, it was shown that the phantom, affine, Mooney-Rivlin, and eight-chain models do not capture the salient features of the reduced-stress behavior for both NR and PDMS. That is, the experiments show a behavior such that the reduced stress increases through a maximum in going from small values of reciprocal deformation ($1/\lambda \sim 0$ or $\lambda \sim \infty$) and then decreases slightly as one moves to greater values of compression. The maximum seems to occur at a value of $1/\lambda \approx 1.5$. The liquidlike model captures some of this but does not exhibit a maximum. Both the constrained chain model and the localization model capture the full range of dry-state behaviors. Important in this assessment is the finding that the eight-chain model exhibits a rapid upturn in $[f^*]$ as the tensile deformation increases from $1/\lambda = 1$. Such behavior is attributed to the early onset of finite chain extensibility in the model but is entirely unrealistic for real rubber. (We note, however, that such behavior may be exhibited by filled rubber [5]).

In the swollen state, it is found that only the constrained chain and localization models capture the decrease in the value of $[f^*]$ as the degree of swelling increases. In fact, the affine, phantom, and liquidlike models exhibit no dependence of the reduced stress on the degree of swelling. Although the Mooney-Rivlin and the eight-chain models show decreasing reduced stress with increasing degree of swelling, their unrealistic dry-state features remain unchanged.

In summary, the constrained chain and localization models do a good job of describing the dry and swollen state stress-strain behaviors of NR and PDMS. The constrained chain model, however, provides a better representation of the swollen state stress-deformation behavior but

is more cumbersome to use. The affine and phantom models are neo-Hookean and do not capture the maximum in the reduced stress in the Mooney-Rivlin representation of the data, nor do they capture the decreasing values of $[F^*]$ as the network is swollen. The Mooney-Rivlin phenomenological model shows a linearly increasing value of $[F^*]$ as one goes from $1/\lambda \sim 0$ (infinite elongation) to $1/\lambda \rightarrow \infty$, whereas in the weakly stretched swollen state, it correctly shows the decreasing reduced stress with increasing degree of swelling. The liquidlike model captures part of the dry-state behavior but does not go through a maximum in $[F^*]$. It also shows no change in $[F^*]$ as the degree of swelling changes.

Finally, the eight-chain model of [3] exhibits a completely different set of behaviors from the other models. It shows a minimum in the Mooney-Rivlin plot that is contrary to the experimentally observed behaviors of NR and PDMS in the dry or swollen states.

APPENDIX

A1. Definition of Reduced Stress

The tensile force along the i-direction, f_I, is equal to the change in the elastic contribution to the Helmholtz free energy, $\Delta F^*_{el,d}$, per unit increase in length, L_i, of the specimen [17] such that

$$f_i = \frac{\partial \Delta F^*_{el,d}}{\partial L_i} = \left(\frac{1}{L_{i,d}}\right) \frac{d\Delta F^*_{el,d}}{\partial \lambda_i}, \tag{46}$$

where $L_{i,d}$ and λ_i are the initial length of the sample and the extension ratio, respectively. Therefore, the true stress, force per unit cross-sectional area $(A_{i,d})$, is given as follows:

$$\begin{aligned} \sigma_i &= \left(\frac{1}{L_{i,d}}\right) \frac{\partial \Delta F^d_{el,d}}{\partial \lambda_i} A^{-1}_{i,d} - p \\ &= \left(\frac{1}{L_{i,d}}\right) \frac{\partial \Delta F^*_{el,d}}{\partial \lambda_i} \left(\frac{L_i}{V_d}\right) - p \\ &= \lambda_i \frac{\partial \Delta F^*_{el,d}}{\partial \lambda_i} \left(\frac{1}{V_d}\right) - p, \end{aligned} \tag{47}$$

where p is the hydrostatic pressure. If the material is assumed, as usual for rubbers, to be incompressible, the sample volume V_d is constant. Subsequently, the true principal stress difference, $\sigma_1 - \sigma_2$, can be written as follows:

$$\sigma_1 - \sigma_2 = \lambda_1 \frac{\partial \left(\frac{\Delta F^*_{el,d}}{V_d}\right)}{\partial \lambda_1} - \lambda_2 \frac{\partial \left(\frac{\Delta F^*_{el,d}}{V_d}\right)}{\partial \lambda_2}$$

$$= \lambda_1 \frac{\partial \Delta F_{el,d}}{\partial \lambda_1} - \lambda_2 \frac{\partial \Delta F_{el,d}}{\partial \lambda_2}, \tag{48}$$

where $\Delta F_{el,d}$ is the free energy density.

When the sample swells in a solvent, the unstretched initial length ($L_{i,d}$) in the dry state changes to the swollen state length ($L_{i,s}$). In this case, the true stress, force per unit swollen and stretched cross-sectional area ($A_{i,s}$) is given as follows:

$$\begin{aligned}
\sigma_i &= \frac{\partial \Delta F^*_{el,s}}{\partial L_i} A^{-1}_{i,s} - p = \left(\frac{1}{L_{i,s}}\right) \frac{\partial \Delta F^*_{el,s}}{\partial \alpha_i} A^{-1}_{i,s} - p \\
&= \left(\frac{1}{L_{i,s}}\right) \frac{\partial \Delta F^*_{el,s}}{\partial \alpha_i} \left(\frac{L_i}{V_s}\right) - p \\
&= \alpha_i \frac{\partial \Delta F^*_{el,s}}{\partial \alpha_i} \left(\frac{1}{V_s}\right) - p,
\end{aligned} \tag{49}$$

where $\Delta F^*_{el,s}$ and V_s are the free energy for the swollen sample and the volume of the swollen sample, respectively. We used the following relation for the extension ratio α_i:

$$\alpha_i = \frac{L_i}{L_{i,s}} = \frac{L_i}{L_{i,d}} \left(\frac{L_{i,d}}{L_{i,s}}\right) = \lambda_i v_p^{1/3} = \lambda_i \lambda_s^{-1}, \tag{50}$$

where v_p and λ_s are the polymer volume fraction and the swelling strain, respectively. We assume that the functional form of the free energy in the swollen state is

$$\Delta F_{el,s}\left(\lambda_s \alpha_i\right) = v_p \Delta F_{el,d}\left(\lambda_i\right). \tag{51}$$

Therefore, we obtain the following expression for the principal stress difference:

$$\begin{aligned}
\sigma_1 - \sigma_2 &= \alpha_1 \frac{\partial \left(\frac{\Delta F^*_{el,s}}{V_s}\right)}{\partial \alpha_1} - \alpha_2 \frac{\partial \left(\frac{\Delta F^*_{el,s}}{V_s}\right)}{\partial \alpha_2} \\
&= \alpha_1 \frac{\partial \Delta F_{el,s}}{\partial \alpha_1} - \alpha_2 \frac{\partial \Delta F_{el,s}}{\partial \alpha_2} \\
&= v_p \left(\alpha_1 \frac{\partial \Delta F_{el,d}}{\partial \alpha_1} - \alpha_2 \frac{\partial \Delta F_{el,d}}{\partial \alpha_2}\right),
\end{aligned} \tag{52}$$

where $\Delta F_{el,s}$ is the free energy density function in the swollen state. When the free energy density function is described in terms of a sum of stretch ratio products of the mth order, there is no swelling dependence of the reduced stress when defined as follows:

$$[f^*] = \frac{(\sigma_1 - \sigma_2)}{\alpha^2 - \frac{1}{\alpha}} \nu_p^{\frac{m}{3}-1}. \tag{53}$$

Throughout this study, we used equation (53) with $m = 2$, which is equivalent to the equation developed by Van der Hoff [45]. In this case, the reduced stress shows no swelling dependence for the phantom, affine, and liquidlike models. We add that equation (53) is not the only definition for reduced stress in the swollen state that could be chosen. The point of interest was the lack of swelling dependence for some models. From a strictly experimental point of view, it would seem natural to simply eliminate the volume fraction term from equation (53). We follow equation (53) for historical reasons.

A2. Reduced Stress in the Swollen State for the Mooney-Rivlin Model

To provide an example of the calculation of the reduced stress in the swollen state, we use the above procedures for the Mooney-Rivlin free energy function. The principal stress difference for the Mooney-Rivlin model is given by

$$\begin{aligned}
\sigma_1 - \sigma_2 &= \nu_p \left(\lambda_s^2 C_0 \left(2\alpha_1^2 - 2\alpha_2^2\right) + \lambda_s^{-2} C_1 \left(-2\alpha_1^{-2} + 2\alpha_2^{-2}\right)\right) \\
&= 2\nu_p \left(\lambda_s^2 C_0 \left(\alpha_1^2 - \alpha_1^{-1}\right) + \lambda_s^{-2} C_1 \left(-\alpha_1^{-2} + \alpha_1\right)\right) \\
&= 2\nu_p^{1/3} \left(\alpha_1^2 - \alpha_1^{-1}\right) \left(C_0 + \nu_p^{4/3} \frac{C_1}{\alpha_1}\right).
\end{aligned} \tag{54}$$

Then, the swollen state reduced stress [45] is

$$[f^*] = 2\left(C_0 + \nu_p^{4/3} \frac{C_1}{\alpha_1}\right). \tag{55}$$

A3. Glossary of Network Structure Parameters

μ = total number of junctions at which the number of chains f is joined together
f = the number of chains joining at a junction, also called the functionality of the junction
ν = total number of chains between neighboring junctions in a network
ξ = independent number of cyclic paths, also called the cyclic rank of a network (in the phantom model, this is the only parameter to describe the elasticity of a network)

The network structure parameters listed above are related through the following equations for perfect networks in which no dangling chains or loops exist and no junctions have a functionality of less than three:

$$\mu = 2\frac{\nu}{f} \quad \xi = \left(1 - \frac{2}{f}\right)\nu \quad \frac{\xi}{V_0} = \left(1 - \frac{2}{f}\right)\rho \frac{N_A}{M_c}, \tag{56}$$

where V_0, ρ, N_A, and M_c are, respectively, the volume, density, Avogadro's number, and the molecular weight of a chain between neighboring junctions [13, 33].

REFERENCES

[1] Allen, G., Kirkham, M. J., Padget, J., and Price, C.: Thermodynamics of rubber at constant volume. *Trans. Faraday Soc.*, 67, 1278 (1971).

[2] Arruda, E. M. and Boyce, M. C.: Evolution of plastic anisotropy in amorphous polymers during finite straining. *Int. J. Plast.*, 9, 697 (1993).

[3] Arruda, E. M. and Boyce, M. C.: A three-dimensional constitutive model for the large stretch behavior of rubber elastic materials. *J. Mech. Phys. Solids*, 41, 389 (1993).

[4] Besseling, J. and van der Giessen, E.: *Mathematical Modelling of Inelastic Deformations, Chapman* Hall, London, 1994.

[5] Bradley, G. L.: Determination of the ultimate capacity of elastomeric bearings under axial loading. Master's thesis, University of Maryland, College Park, 1997.

[6] Deam, R. T. and Edwards, S. F.: The theory of rubber elasticity. *Phil. Trans. Roy. Soc.* London, A, 280, 317 (1978).

[7] DiMarzio, E. A.: Contribution to a liquid-like theory of rubber elasticity. *J. Chem. Phys.*, 36, 1563 (1962).

[8] DiMarzio, E. A.: Contribution to a liquid-like theory of rubber elasticity: 2. Existence of a $(\lambda_x\lambda_y + \lambda_y\lambda_z + \lambda_z\lambda_x)$ term. *Polymer*, 35, 1819 (1994).

[9] Douglas, J. F. and McKenna, G. B.: The effect of swelling on the elasticity of rubber: Localization model description. *Macromolecules*, 26, 3282 (1993).

[10] Edwards, S. F.: The theory of rubber elasticity. *Brit. Polym. J.*, 9, 140 (1977).

[11] Erman, B. and Mark, J. E.: Interpretation of stress-strain isotherms for elastomers cross linked in solution. *Macromolecules*, 20, 2892 (1987).

[12] Erman, B. and Mark, J. E.: Stress-strain isotherms for elastomers cross linked in solution. 2. Interpretation in terms of the constrained chain model. *Macromolecules*, 25, 1919 (1992).

[13] Erman, B. and Mark, J. E.: *Structure and Properties of Rubberlike* Networks, Oxford University Press, New York, 1997.

[14] Erman, B. and Monnerie, L.: Theory of elasticity of amorphous networks: Effect of constraints along chains. *Macromolecules*, 22, 3342 (1989).

[15] Erman, B. and Monnerie, L.: Corrections. *Macromolecules*, 25, 4456 (1992).

[16] Ferry, J. D.: *Viscoelastic Properties of Polymers*, Wiley, New York, 1980.

[17] Flory, P. J.: *Principles of Polymer Chemistry*, Cornell University Press, Ithaca, NY, 1953.

[18] Flory, P. J.: Theory of elasticity of polymer networks: The effect of local constraints on junctions. *J. Chem. Phys.*, 66, 5720 (1977).

[19] Flory, P. J. and Erman, B.: Theory of elasticity of polymer networks. *Macromolecules*, 15, 800 (1982).

[20] Flory, P. J. and Rehner, J.: Statistical mechanics of cross-linked polymer networks. *J. Chem. Phys.*, 11, 521 (1943).

[21] Flory, P. J. and Tatara, Y: The elastic free energy and the elastic equation of state: Elongation and swelling of polydimethylsiloxane networks. *J. Polym. Sci., Polym. Phys. Ed.*, 13, 683 (1975).

[22] Frenkel, J.: A theory of elasticity, viscosity and swelling in polymeric rubber-like substances. *Rubber Chem. Tech.*, 13, 264 (1940).

[23] Gaylord, R. J. and Douglas, J. F.: Rubber elasticity: A scaling approach. *Polym. Bull.*, 18, 347 (1987).

[24] Gaylord, R. J. and Douglas, J. F.: The localisation model of rubber elasticity. *Polym. Bull.*, 23, 529 (1990).

[25] Gottlieb, M. and Gaylord, R. J.: Experimental tests of entanglement models of rubber elasticity: 1. Uniaxial extension-compression. *Polymer*, 24, 1644 (1983).

[26] Gottlieb, M. and Gaylord, R. J.: Experimental tests of entanglement models of rubber elasticity: 2. Swelling. *Macromolecules*, 17, 2024 (1984).

[27] Graessley, W. W.: Entangled linear, branched and network polymer systems: Molecular theories. *Adv. Polym. Sci.*, 47, 67 (1982).

[28] Haward, R. N.: Strain hardening of thermoplastics. *Macromolecules*, 26, 5860 (1993).

[29] Hermans, J. J.: Deformation and swelling of polymer networks containing comparatively long chains. *Trans. Faraday Soc.*, 43, 591 (1947).

[30] Higgs, P. G. and Ball, R. C.: Trapped entanglements in rubbers. A unification of models. *Europhys. Lett.*, 8, 357 (1989).

[31] Higgs, P. G. and Gaylord, R. J.: Slip-links, hoops and tubes: Tests of entanglement models of rubber elasticity. *Polymer,* 31, 70 (1990).

[32] James, H. M. and Guth, E.: Theory of elastic properties of rubber. *J. Chem. Phys.,* 11, 455 (1943).

[33] James, H. M. and Guth, E.: Statistical thermodynamics of rubber elasticity. *J. Chem. Phys.,* 15, 669 (1947).

[34] Mark, J. E. and Erman, B.: *Rubberlike Elasticity: A Molecular Primer,* Wiley-Interscience, New York, 1988.

[35] McKenna, G. B. and Hinkley, J. A.: Mechanical and swelling behavior of well characterized polybutadiene networks. *Polymer,* 27, 1318 (1986).

[36] Mooney, M.: A theory of large elastic deformation. *J. Appl. Phys.,* 11, 582 (1940).

[37] Mullins, L.: Determination of degree of crosslinking in natural rubber vulcanizates: Part IV Stress-strain behavior at large extensions. *J. Appl. Polym. Sci.,* 2, 257 (1959).

[38] Pak, H. and Flory, P. J.: Relationship of stress to uniaxial strain in crosslinked poly(dimethylsiloxane) over the full range from large compression to high elongations. *J. Polym. Sci., Polym. Phys. Ed.,* 17, 1845 (1979).

[39] Rivlin, R. S.: Elastic deformations of isotropic materials. *Phil. Trans. Roy. Soc.* London, A, 240, 459 (1948).

[40] Rivlin, R. S. and Saunders, D. W.: Large elastic deformations of isotropic materials: VII. Experiments on the deformation of rubber. *Phil. Trans. Roy. Soc.* London, A, 243, 251 (1951).

[41] Ronca, G. and Allegra, G.: An approach to rubber elasticity with internal constraints. *J. Chem. Phys.,* 63, 4990 (1975).

[42] Rubin, M. B.: Plasticity theory formulated in terms of physically based microstructural variables. *Int. J. Solids Struct.,* 31, 532 (1994).

[43] Tervoort, T. A.: Constitutive modelling of polymer glasses: Finite, nonlinear viscoelastic behaviour of polycarbonate. Doctoral thesis, Technische Univeriteit Eindhoven, CIP-GGegevens Koninklijke Bibliotheek, den Haag, the Netherlands, 1996.

[44] Treloar, L.R.G.: The photoelastic properties of short-chain molecular networks. *Trans. Faraday Soc.,* 50, 881 (1954).

[45] Van der Hoff, B.M.E.: The stress strain relation of swollen rubbers. *Polymer,* 6, 397 (1965).

[46] Varga, O. H.: *Stress-Strain Behavior of Elastic Materials: Selected Problems of Large Deformations,* Interscience, New York, 1966.

[47] Wall, F. T.: Statistical thermodynamics of rubber. *J. Chem. Phys.,* 11, 527 (1943).

[48] Wang, M. C. and Guth, E.: Statistical theory of networks of non-Gaussian flexible chains. *J. Chem. Phys.,* 20, 1144 (1952).

[49] Wu, P. D. and van der Giessen, E.: On improved network models for rubber elasticity and their applications to orientation in glassy polymers. *J. Mech. Phys. Solids,* 41, 427 (1993).